Mechanical Responses of the Organ of Corti to Acoustic and Electrical Stimulation In Vitro

Dylan K. Chan and A. J. Hudspeth
Howard Hughes Medical Institute and Laboratory of Sensory Neuroscience, The Rockefeller University, New York, New York

ABSTRACT The detection of sound by the cochlea involves a complex mechanical interplay among components of the cochlear partition. An in vitro preparation of the second turn of the jird's cochlea provides an opportunity to measure cochlear responses with subcellular resolution under controlled mechanical, ionic, and electrical conditions that simulate those encountered in vivo. Using photodiode micrometry, laser interferometry, and stroboscopic video microscopy, we have assessed the mechanical responses of the cochlear partition to acoustic and electrical stimuli near the preparation's characteristic frequency. Upon acoustic stimulation, the partition responds principally as a rigid plate pivoting around its insertion along the spiral lamina. The radial motion at the reticular lamina greatly surpasses that of the tectorial membrane, giving rise to shear that deflects the mechanosensitive hair bundles. Electrically evoked mechanical responses are qualitatively dissimilar from their acoustically evoked counterparts and suggest the recruitment of both hair-bundle- and soma-based electromechanical transduction processes. Finally, we observe significant changes in the stiffness of the cochlear partition upon tip-link destruction and tectorial-membrane removal, suggesting that these structures contribute considerably to the system's mechanical impedance and that hair-bundle-based forces can drive active motion of the cochlear partition.

INTRODUCTION

The cochlear partition, which comprises the basilar membrane, organ of Corti, and tectorial membrane, plays a critical role in auditory transduction. Through its complex mechanical properties, this structure transforms sound-induced intracochlear pressure gradients into forces that deflect hair bundles atop mechanoreceptive hair cells. The precise manner in which the cochlear partition moves is poorly understood, though, as are its underlying micromechanical properties. Modeling on the basis of the limited experimental data available and a priori principles derived from the partition's microscopic structure has yielded diverse results (1). Whereas simple models yield unimodal, drumhead-like motions across the width of the cochlear partition, models that invoke additional resonances of the tectorial membrane or other structures within the cochlear partition exhibit a more complex behavior. Direct measurements by laser interferometry of the detailed features of cochlear-partition movement in response to acoustic stimuli have produced similarly ambiguous results (2). Although some studies have corroborated models of unimodal motion (3–5), others have revealed dramatic phase differences across the basilar membrane (6). Furthermore, none of these in vivo experiments has been able to measure directly the relative movements of the basilar membrane, tectorial membrane, and reticular lamina under acoustic stimulation, even though these motions produce the shearing forces that drive hair-bundle deflection. Finally, laser interferometry cannot provide access to the internal structures of the organ of Corti, including the hair bundles themselves.

Electrical stimulation of excised preparations in vitro has been used to explore the internal micromechanics of the organ of Corti in greater detail than is possible in vivo (7–10). Such an investigation first provided evidence for opposing movement of the reticular lamina and basilar membrane (11), supporting a role for somatic electromotility in electromechanical feedback. In general, electrically evoked movements of the cochlear partition have been interpreted as manifestations of the electromechanical reverse limb of the cochlear active process. Despite some evidence that such motions behave like their acoustically stimulated counterparts (12), however, the precise motions that electrical stimuli elicit are unclear, as is their relevance to amplification in vivo.

A recently developed in vitro preparation of the jird's cochlea provides an opportunity to observe cochlear movements at moderate frequencies in response to both acoustic and electrical stimulation (13,14). Because the cochlear partition in this preparation remains suspended as it does in vivo, its mechanical boundary conditions, at least across the radial dimension, resemble those in an intact animal. In addition, this preparation allows direct measurement of the stiffnesses of the cochlear partition and its constituent components in response to realistic pressure stimuli. We have used a combination of photodiode-based displacement measurement, laser interferometry, and stroboscopic video microscopy to examine the micromechanical properties of an excised segment of the cochlear partition as it responds near its characteristic frequency.

Submitted July 13, 2005, and accepted for publication September 8, 2005.

Address reprint requests to Dr. A. J. Hudspeth, Howard Hughes Medical Institute and Laboratory of Sensory Neuroscience, Box 314, The Rockefeller University, 1230 York Ave., NY, NY 10021-6399. Tel.: 212-327-7351; Fax: 212-327-7352; E-mail: hudspaj@rockefeller.edu.

0006-3495/05/12/4382/14 $2.00

doi: 10.1529/biophysj.105.070474

MATERIALS AND METHODS

In vitro preparation of the jird's cochlea

Experiments were performed on Mongolian clawed jirds (*Meriones unguiculatus*), which as members of the Subfamily Gerbillinae are also known as gerbils (15). An animal 3–6 weeks of age was injected with a single intraperitoneal bolus of 200 mg · kg^{-1} sodium pentobarbital (Nembutal, Abbott Laboratories, Abbott Park, IL). After the corneal reflex and response to tail pinch had vanished, the animal was decapitated. The intact auditory bullae were isolated by using a number 20 scalpel blade to bisect the ventral floor of the skull, transect the temporomandibular joint, and reflect the bullae posteroventrally. Once removed, the bullae were immersed in oxygenated dissecting solution containing 145 mM NaCl, 3 mM KCl, 250 μM $CaCl_2$, 250 μM $MgCl_2$, 2 mM sodium pyruvate, 5 mM D-glucose, and 10 mM Na_2HPO_4 at pH 7.3.

Each bulla was opened by chipping away its bony wall with coarse forceps, forming a 1.5-mm-wide, 3-mm-long, anterior-to-posterior opening in the anterior aspect of the ventral wall. The lateral wall of the bulla, including the bony structure housing the tympanic membrane, was then reflected laterally and discarded; this exposed the cochlea, which sits on the anteromedial wall of the bulla embedded in the temporal bone. The remaining attached bone, the bulla's anterior wall, was removed at the joint with the bony outer wall of the cochlea, freeing the anterior surface of the cochlea of extraneous bone.

The apical two turns of the cochlea were isolated by making a planar, circumferential cut through the basal turn, orthogonal to the modiolar axis. The modiolus was first transected basal to the middle turn with a #11 scalpel blade inserted into the internal auditory meatus. The same blade was then used to cut through the lateral bony wall of the cochlea just basal to the junction between the middle and basal cochlear turns. To complete the cochlear transection, the scalpel was used to score and finally cut through the temporal bone flanking the internal auditory meatus. The apical two turns thus isolated were then transferred to fresh dissecting solution.

The cochlear fragment was next mounted on a plastic disk made by punching a 12.5-mm circular disk from a 250-μm-thick plastic coverslip (Fisherbrand, Pittsburgh, PA) and boring a 1.8-mm-diameter hole in its center. To render the experimental preparation as flat as possible, the cut aspect of the cochlea was trimmed of bony protrusions. The cochlear fragment was then placed, basal-side-down, atop the hole in the mounting disk so that the outer bony wall of the fragment contacted the plastic disk. After excess fluid had been wicked off, biocompatible cyanoacrylate glue (Iso-Dent, Ellman International, Oceanside, NY) was applied liberally to the interface between the disk and the outer cochlear wall. The glue was made to polymerize by reapplying dissecting solution to the specimen.

The mounted cochlea was transferred to a fresh dish and cleaned of excess glue. It was positioned with the apical end pointing downward to allow access to the ceiling of the scala vestibuli in the basal turn, which was visible through the hole in the mounting disk. This ceiling, which separated the basal from the middle turn, was chipped away with fine forceps, exposing the basal aspect of the cochlear partition in the middle turn.

To isolate completely the apical and basolateral epithelial surfaces of the organ of Corti, it was necessary to block communication through the spiraling cochlear scalae. We accomplished this by expelling cyanoacrylate glue into four locations from a pulled glass micropipette 30–50 μm in tip diameter. The scala tympani of the middle turn, peripheral to the newly exposed segment of basilar membrane, was blocked completely in both the apical and basal directions. The scala vestibuli of the basal turn was likewise sealed with glue, as was the opening of the modiolus. In this way, all leakage paths between the basal and apical aspects of the epithelium were obstructed.

To expose the apical aspect of the epithelium, the mounted preparation was placed with the apical end facing up. The bone near the helicotrema was chipped away with fine forceps to make a small hole. The bony lateral wall of the apical turn was then reflected outward and removed. The stria vascularis and the cochlear partition of the apical turn were removed, exposing the floor of the scala tympani. To reveal the apical aspect of the middle turn, the bone forming this floor, which separated the apical and middle turns, was chipped away, together with the upper half of the lateral wall of the middle turn. Once exposed, Reissner's membrane of the middle turn was removed with a glass micropipette. When indicated, we used the broken end of a glass micropipette with a tip diameter of ~20 μm to lift the tectorial membrane and retract it toward the longitudinal ends of the preparation.

Experimental chamber

The experimental system consisted of a two-compartment recording chamber coupled to an earphone. The acoustic path from the earphone included 20 mm of Tygon tubing, with a 1.6-mm internal diameter and 4.8-mm external diameter, connected to a three-way valve for pressure release; a 265-mm length of low-compliance plastic tubing; and a 10-mm length of Tygon tubing coupled to the lower compartment of the recording chamber. This lower compartment comprised a 15-mm-long channel, 1.3 mm × 0.8 mm in cross-section, ending in a cylindrical segment 1.8 mm in diameter and 1 mm high. Leading into this terminal segment were two side channels, each 11 mm in length, that housed Ag-AgCl electrodes embedded in 2% (weight/volume) agarose in dissecting solution.

The completed preparation was sealed onto the recording chamber with vacuum grease. The preparation was ordinarily oriented with the apical surface facing up. To record interferometrically from the basilar membrane, it was usually necessary to mount the preparation with the apical end facing down; this required the use of a similar recording chamber with a larger terminal segment that was 5 mm in diameter. A plastic ring was placed around the edge of the plastic disk to secure the preparation. The lower compartment was flushed and filled with oxygenated artificial perilymph (145 mM NaCl, 3 mM KCl, 1.3 mM $CaCl_2$, 0.9 mM $MgCl_2$, 2 mM sodium pyruvate, 5 mM D-glucose, and 10 mM Na_2HPO_4 at pH 7.3), and a plastic coverslip was sealed onto the lower face of the chamber with vacuum grease. Air bubbles and excess perilymph were removed from the lower compartment through a fine tube inserted into the acoustic port, leaving only enough perilymph—typically 2–4 μl—to fill the terminal cylindrical chamber. After the acoustic port leading to the lower compartment had been coupled to the earphone tube, the pressure-release valve was closed. The solution in the upper compartment was then flushed and replaced with oxygenated artificial endolymph containing 150 mM *N*-methyl-D-glucamine (NMDG), 25 μM $CaCl_2$, 1 mM sodium pyruvate, 5 mM D-glucose, and 10 mM H_3PO_4 at pH 7.3. This solution, which differs from physiological endolymph most significantly in its content of NMDG instead of K^+ as the primary monovalent cation, supports nonlinear amplification and electrically evoked motion of the cochlear partition that are indistinguishable from those elicited in the presence of K^+-based endolymph (13). The NMDG–based solution was used throughout this study because it allowed each preparation to remain healthy for a longer recording period, ~45–60 min. Because we did not impose an endocochlear potential in these measurements, the observed mechanical properties represent the cochlear partition's passive response to acoustic stimulation.

Acoustic stimulation and calibration

The earphone used to present acoustic stimuli (ER-2, Etymotic Research, Elk Grove Village, IL) was driven by an amplifier (AM 502, Tektronix, Beaverton, OR) connected to the experimental computer (Precision 650, Dell, Round Rock, TX). To compensate for irregularities in the frequency response of the system, we measured the pressure with a transducer (8507C-1, Endevco, San Juan Capistrano, CA) in place of the specimen. The computer-generated stimuli were then adjusted to ensure constant amplitudes at all frequencies (13).

The magnitudes of all stimuli are reported as sound-pressure levels (SPLs) measured in an aqueous medium with reference to a root-mean-square pressure of 20 μPa. Because the middle ear enhances sound pressures ~10-fold, the reported values are ~20 dB greater than the corresponding sound-pressure levels for airborne stimuli presented to an intact animal (14,16).

Nomenclature and sign conventions

When referring to the cochlear partition, we include the basilar membrane, organ of Corti, and tectorial membrane. Because it is thought to have a negligible mechanical resistance and was removed in our dissections, Reissner's membrane is not included in this definition. Throughout this work, upward vertical motion of surfaces is defined as movement toward the upper compartment of the experimental preparation, which corresponds to the scala vestibuli of the intact cochlea. Such responses are plotted as positive values in the relevant traces and graphs and are used as such for phase analyses. Inward radial motion of structures along the reticular lamina refers to their displacement toward the spiral lamina and modiolus. Because these *inward* movements produce shear with respect to the radially stationary undersurface of the tectorial membrane that deflects hair bundles *outward* toward the tallest rows of stereocilia, such motions are reported as positive values in the relevant traces and graphs.

Measurement of radial and vertical movements

The radial displacements of structures at the reticular lamina were measured with a photodiode projection system as described (13). Laser Doppler velocimetry was used to detect vertical motion of the tectorial membrane and basilar membrane. The laser beam of a heterodyne interferometer (OFV 501, Polytec, Tustin, CA) was directed to the sample through the fluorescence port of an upright microscope (MPS, Zeiss, Thornwood, NY) by means of a custom-built coupler that permitted translation and tilt of the interferometer's probe head. The laser beam was focused onto the sample through the same ×40 water-immersion objective used for bright-field imaging. A partially silvered mirror in the laser beam's path permitted simultaneous bright-field imaging and visualization of the laser spot, which was adjusted to a diameter of ~10 μm. Glass beads 20-μm in diameter were placed atop the preparation, which was then moved under microscopic observation so that a bead maximally reflected the laser beam. The position of the bead was noted with reference to the structure of the organ of Corti directly below it. Five or six beads were typically distributed at varying locations across the radial dimension of the exposed cochlear segment over 80–100 μm of its longitudinal extent, a range over which displacements at the same radial location are similar to within 20%.

Stroboscopic video microscopy

Stroboscopic videos of cochlear motion were obtained at acoustic frequencies. Illumination was provided by a green light-emitting diode (Luxeon Star, Lumileds, San Jose, CA) driven by 7-V, square-pulse trains with an on/off duty-cycle of 1:10. By stimulating with an acoustic tone or a sinusoidal electrical current (13) at a frequency that differed from that of illumination by 1–2 Hz, we obtained strobed videos of the resulting movement. Such videos were recorded at specific focal depths, controlled by a *z*-axis stepping-motor drive (Prior Scientific, Rockland, MD), and processed with commercial software (Premiere Pro, Adobe Systems, San Jose, CA). To assess the direction and magnitude of motion within the cochlear partition, optical flow determinations were performed with an algorithm (17) in the FlowJ program (18). The parameters used to determine the spatial and temporal properties of the analysis were as follows: σ_S, the dimensionless space constant for velocity determination; σ_T, the dimensionless time constant for velocity determination; τ, the threshold for velocity detection (pixel $\cdot$ s^{-1}); σ_W, the dimensionless space constant over which velocities were constrained to be regular; and ρ, the saturation point of the pseudocolor scale (pixel $\cdot$ s^{-1}).

Stiffness measurement

The stiffness of the cochlear partition was calculated from principles described earlier (13). Unlike the situation in vivo, in which only a small boundary layer of fluid directly adjacent to the cochlear partition participates in its movement (16), vibration of the cochlear partition in this experimental configuration entrains a larger volume of perilymph. Coupled to the mass m of perilymph that moves with the cochlear partition, the segment of cochlear partition with stiffness K constitutes a second-order harmonic oscillator whose resonant frequency ω_0 is

$$\omega_0 = \sqrt{\frac{K}{m}}. \tag{1}$$

The value of the relevant mass can be estimated by measuring the length, and thus the volume, of the column of perilymph entrained by the partition's motion. Consider a lower compartment whose arbitrary cross-sectional area, $A(z)$, may vary along its length, the z axis. Let $z = 0$ denote the position of the air-perilymph interface at the bottom of the liquid column and $z = Z$ that of the cochlear partition. Assume that all movements of the liquid are parallel to the z axis. During presentation of a time-dependent pressure stimulus $P(t)$, the cochlear partition moves a distance $\bar{X}(Z,t)$ averaged across its distensible surface area. The force applied at the air-perilymph interface must thus accelerate the entrained column of liquid and deflect the cochlear partition. Disregarding the effect of viscous drag, the equation of motion is then

$$P(t)A(0) = \frac{d}{dt}\left[\int_0^Z \rho A(z)v(z,t)dz\right] + K\bar{X}(Z,t), \tag{2}$$

in which ρ is the density of the liquid and $v(z,t)$ the velocity of an element of the liquid at position z and time t. Because the liquid is incompressible and moves only along the z axis, the volume velocity at every vertical position must be the same:

$$A(z)v(z,t) = A(Z)v(Z,t). \tag{3}$$

Substitution then yields

$$\begin{aligned} P(t)A(0) &= \frac{d}{dt}\left[\int_0^Z \rho A(Z)v(Z,t)dz\right] + K\bar{X}(Z,t) \\ &= \rho A(Z)Z\frac{dv(Z,t)}{dt} + K\bar{X}(Z,t). \end{aligned} \tag{4}$$

For sinusoidal stimulation, the pressure is of the form $P(t) = pe^{i\omega t}$, and we anticipate a response at the cochlear partition of the form $\bar{X}(t) = xe^{i(\omega t+\phi)}$; the equation of motion and its solution are therefore

$$P(t)A(0) = -\omega^2\rho A(Z)Z\bar{X}(Z,t) + K\bar{X}(Z,t);$$

$$\bar{X}(Z,t) = \frac{-P(t)A(0)}{\rho A(Z)Z\left[\omega^2 - \dfrac{K}{\rho A(Z)Z}\right]} = \frac{-P(t)\left[\dfrac{A(0)}{A(Z)}\right]}{\rho Z(\omega^2 - \omega_0^2)}, \tag{5}$$

in which

$$\omega_0 = \sqrt{\frac{K}{\rho A(Z)Z}}. \tag{6}$$

We confirmed the validity of this approach by conducting a control experiment in which the cochlear partition was replaced in the recording apparatus by a thin film of cyanoacrylate glue. The stiffness value calculated from the observed resonant frequencies agreed with those determined by the application of static or low-frequency pressure changes.

For a typical excised segment of the cochlear partition ~700 μm long and 200–250 μm across, the distensible area, $A(Z)$, was ~0.16 mm^2. The area of the air-perilymph interface at which the acoustic pressure stimulus was applied, $A(0)$, measured 1.04 mm^2. The mass of liquid concealed directly under the preparation, and therefore excluded from measurement,

was estimated by linear regression of the resonance frequencies determined for each of several different fluid-column lengths (13). The resonant frequency was measured from the response of the hair bundles on inner hair cells to acoustic frequency sweeps of 300–3000 Hz at 58 dB SPL. Using this mass and the resonant frequency, we calculated the stiffness from the relation immediately above.

Several factors limit the precision of our estimate of the cochlear partition's stiffness. Owing to differences in dissection and in the placement of the cyanoacrylate glue used to seal the scalae, the exposed length of the cochlear partition varied from preparation to preparation. Moreover, the presence of the cement in the scalae may have restricted the motion of the segment's ends. Because viscous drag somewhat damped the oscillation of the cochlear partition, we measured a resonant frequency slightly lower than the natural frequency ω_0. By fitting the observed resonances (e.g., Fig. 7 *C*) with the explicit relation for a damped second-order resonator, we estimated the magnitude of the drag coefficient at 2 $mN \cdot s \cdot m^{-1}$. This value indicates that neglecting the effect of drag introduces an error of ~10% in our estimates of stiffness.

RESULTS

Vertical response of the cochlear partition to acoustic stimuli

We measured the vertical velocities of the tectorial membrane and basilar membrane at various positions across their radial dimension in response to acoustic stimuli. For each set of measurements, 20-μm glass beads were placed either atop the tectorial membrane in a preparation mounted apical-side-up, or on the basilar membrane in the apical-side-down configuration (Fig. 1 *A*). We used laser Doppler velocimetry to measure the vertical velocity, from which we calculated the displacement.

In response to 58-dB SPL sinusoidal stimulation at 700 Hz, the preparation's resonant frequency, the vertical displacement of the tectorial membrane was minimal at the location nearest the spiral lamina (Fig. 1 *B*). The displacement generally increased as the site of measurement progressed radially outward, such that a point atop the Hensen's cells, beyond the outermost extent of the tectorial membrane, exhibited a displacement roughly thrice that above the spiral lamina. This increase in movement was accompanied by a slight but monotonically increasing phase lag, with motion at the Hensen's cells lagging that at the spiral lamina by a maximum of 30° (Fig. 1 *C*).

The vertical velocity of the basilar membrane could be assessed when a preparation was mounted with the apical-end pointing downward. Because the lower compartment of the recording chamber in this configuration was necessarily large, however, it was impossible to achieve a resonant frequency for the preparation as great as the characteristic frequency in vivo or the second-order resonant frequency obtained in the ordinary, apical-side-up configuration.

Stimulation at 1 kHz and 58 dB SPL in the apical-side-down configuration elicited small but measurable motions of the basilar membrane. Like that of the tectorial membrane, the basilar membrane's displacement was minimal at the edge of the spiral lamina and increased in the radial direction (Fig. 1 *D*). A similar phase lag was observed as well, but of larger magnitude: the outermost point measurable, equivalent to the third row of outer hair cells, lagged the innermost point, below the inner hair cells, by ~50° (Fig. 1 *E*). These findings suggest that acoustic stimuli of a moderately high frequency cause the cochlear partition to move for the most part as a rigid plate pivoting along its insertion at the spiral lamina. In both recording configurations, assessment of movement farther radially outward than the boundary between the outer hair cells and Hensen's cells was not possible owing to optical scattering from overlying tissue that precluded laser-interferometric measurements. Because the cochlear partition's insertion at the spiral ligament was stationary, however, the partition's motion necessarily decreased from the region near the Hensen's cells toward the spiral ligament, which is in accordance with models of parabolic, unimodal motion (3–5).

Radial response of the reticular lamina to acoustic stimuli

To assess the shear delivered to the hair bundles, we measured the radial displacement of structures on the reticular lamina in response to acoustic stimulation. Five features at the level of the reticular lamina consistently yielded images with sufficient contrast to permit detection of their motion by the photodiode pair. From the spiral lamina outward, these were the hair bundles of the inner hair cells, the boundary between the inner and outer pillar cells, and the inner edges of each of the three rows of outer hair cells (Fig. 2 *A*). The radial displacement of each of these structures was measured in response to a 300–3000-Hz acoustic stimulus at 58 dB SPL.

In contrast to the vertical response of the cochlear partition, which was minimal at the spiral lamina, the response of the reticular lamina peaked at the hair bundles of inner hair cells and declined monotonically toward the boundary of the third row of outer hair cells, whose displacement was only a quarter of the maximum (Fig. 2 *B*). This decrease in response amplitude toward the outer hair cells was accompanied by a small but monotonic increase in phase lead with distance from the spiral lamina, with the third row of outer hair cells leading the inner hair cells by a maximum of 90° (Fig. 2 *C*).

Because the tectorial membrane does not possess structures with high-contrast edges that are amenable to projection onto the photodiode pair, we imaged glass beads placed atop it. These beads exhibited negligible radial motion at all positions (data not shown), suggesting that the top surface of the tectorial membrane moves almost exclusively in the vertical direction. It follows that the shear between the radially displaced reticular lamina and the radially stationary tectorial membrane deflects the hair bundles. It should be noted that this arrangement confers an apparently paradoxical polarity on hair-bundle displacement, in which the radially inward translation of a hair bundle is associated with the outward deflection of its top toward the tallest row of stereocilia, and therefore with positive stimulation (14).

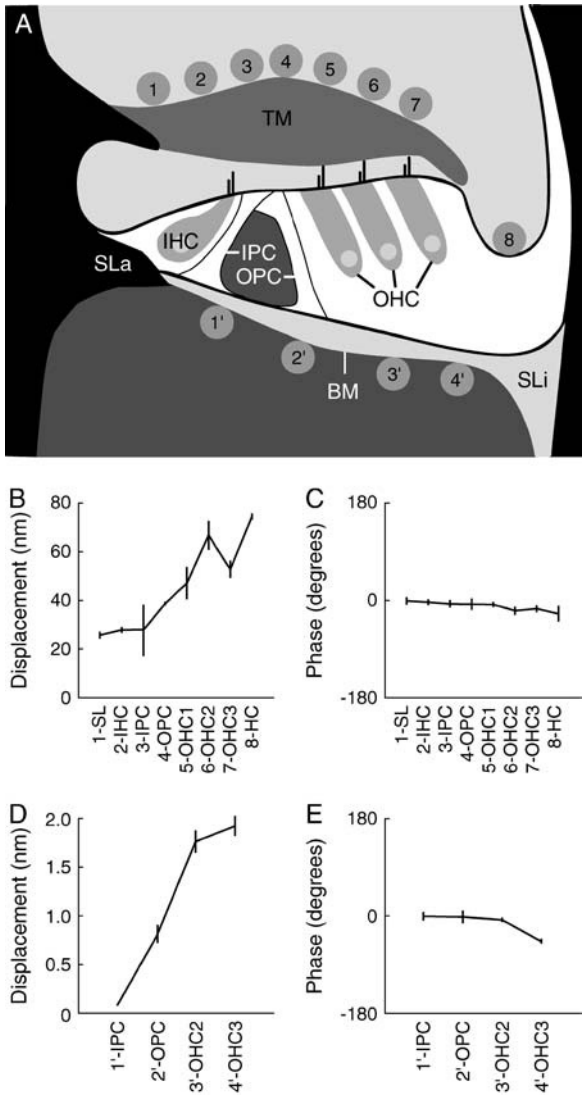

FIGURE 1 Vertical response of the cochlear partition to acoustic stimulation. (*A*) In the in vitro preparation of the jird's cochlea, the cochlear partition is suspended between its natural insertions at the spiral lamina, which forms its inner (modiolar) attachment, and at the spiral ligament, which constitutes its outer boundary. The velocity of glass beads attached to the tectorial and basilar membranes was measured by laser Doppler interferometry. The numbers correspond to the locations indicated in *B–E*. (*B*) In response to a 58-dB SPL acoustic stimulus at 700 Hz, the resonant frequency of this preparation, tectorial-membrane displacement generally increased as a function of distance from the spiral lamina. (*C*) The phase of tectorial-membrane displacement relative to that measured at the innermost point varied only slightly with radial position. (*D*) In response to a 58-dB SPL acoustic stimulus, basilar-membrane displacement also grew with increasing distance from the spiral lamina. Because the preparation was mounted with its apical end down to permit access to the basilar membrane, the stimulus frequency of 1000 Hz significantly exceeded the second-order resonant frequency imposed by the increased volume of perilymph in the lower compartment of the experimental chamber. (*E*) The phase of basilar-membrane displacement relative to the displacement at the innermost point varied little with radial position, except for a phase lag near 50° at the outermost position. In general, the movements of the tectorial and basilar membranes were essentially in phase with one another. Here and in Figs. 2, 4, 5, and 8, the schematic illustration of the cochlear partition exaggerates the 100-μm region of the basilar membrane overlain by the organ of Corti.

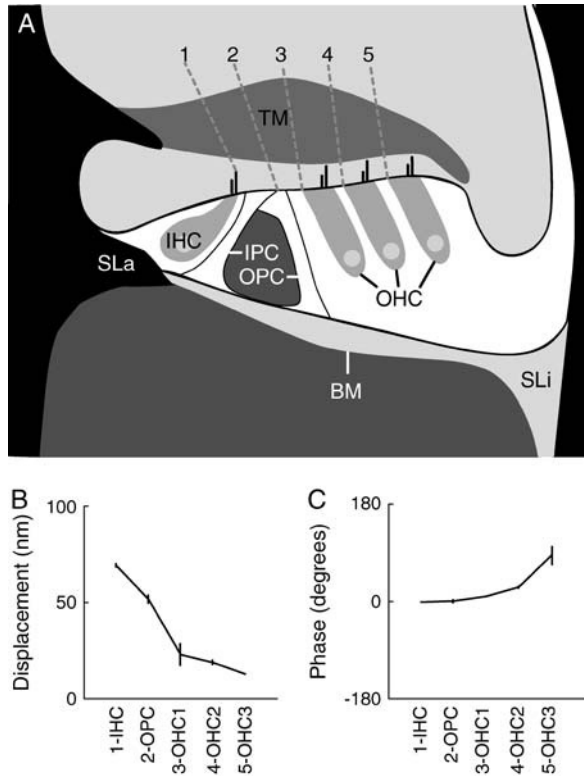

FIGURE 2 Radial response of the reticular lamina to acoustic stimulation. (*A*) The displacements of the cellular structures on the reticular lamina indicated with dashed lines were measured with the photodiode projection system. Numbers correspond to the locations cited in *B* and *C*. (*B*) In response to a 58-dB SPL acoustic stimulus at 800 Hz, the resonant frequency of this preparation, the inward radial displacement of cellular structures at the reticular lamina decreased as a function of distance from the spiral lamina; the greatest displacement was observed for the hair bundles of inner hair cells. (*C*) Points increasingly distant from the spiral lamina exhibited a growing phase lead, with the inner boundary of the third row of outer hair cells leading the hair bundle of an inner hair cell by ~90°. (*BM*, basilar membrane; *IHC*, inner hair cell; *IPC*, inner pillar cell; *OHC*, outer hair cell; *OPC*, outer pillar cell; *SLa*, spiral lamina; *SLi*, spiral ligament; and *TM*, tectorial membrane.) The points and vertical bars in *B* and *C* represent the means and standard deviations of the measurements.

Stroboscopic video microscopy of the acoustically stimulated cochlear partition

Both photodiode micrometry and laser interferometry measure movements at different locations over a period of time, and are thus subject to artifacts of slow drift. Moreover, the former technique is limited to the detection of high-contrast edges. Stroboscopic video microscopy, on the other hand, permits the direct observation of motion throughout the cochlear partition. We therefore recorded videos of the

The additional 100–150 μm of basilar membrane between the Hensen's cells and the spiral ligament was not visible in the preparation and is not depicted to scale. (*BM*, basilar membrane; *HC*, Hensen's cell; *IHC*, inner hair cell; *IPC*, inner pillar cell; *OHC*, outer hair cell; *OPC*, outer pillar cell; *SLa*, spiral lamina; *SLi*, spiral ligament; and *TM*, tectorial membrane.) The points and vertical bars in *B–E* represent the means and standard deviations of the measurements.

mechanical response to 1000-Hz acoustic stimulation at 78 dB SPL under illumination by a light-emitting diode driven with 0.1-ms voltage pulses at ~1002 s^{-1} (Supplementary Material, Fig. S1). This stroboscopic system illuminated 1/10th of each cycle of movement to produce a video of motion with an apparent frequency of ~2 Hz. With the camera's capture rate of 30 frames · s^{-1}, each frame thus recorded a snapshot of ~17% of a cycle.

The stroboscopic video of acoustically evoked movement corroborated the interferometric and photodiode-derived findings. The edges of both the spiral lamina and the spiral ligament, which we could visualize through overlying tissue, were clearly fixed: the suspended cochlear partition vibrated largely as a unit, with no dramatic phase discontinuities. Radial motion was negligible throughout the tectorial membrane, whereas that component was substantial at the reticular lamina, especially near the hair bundles of inner hair cells. The hair bundles would necessarily be deflected by this shear. Our ability to observe deflection of the hair bundles varied between preparations, depending upon the precise angle of mounting and preparation-dependent optical properties. In one exceptional preparation, hair-bundle deflection was readily observable; the tops of the bundles on inner hair cells were virtually stationary as the reticular lamina moved radially below them (Supplementary Material, Fig. S2). Such motion undoubtedly deflected the hair bundles around their insertions at the reticular lamina.

Electrically evoked hair-bundle movement

A 30-μA electrical stimulus in the form of a 300–3000-Hz frequency sweep or a 50-ms pulse elicited hair-bundle movements on inner hair cells up to 60 nm in peak-to-peak magnitude (Fig. 3 *A*). Positive polarization of the upper compartment, which should hyperpolarize the apical surface of a hair cell and depolarize its basolateral membrane (19), produced radially outward displacement of the hair bundle (Fig. 3, *B* and *C*) and downward movement of the tectorial membrane (data not shown). Both of these responses correspond to inward, or negative, deflection of the hair bundle's top. The electrically evoked response declined with increasing stimulus frequency (Fig. 3 *D*) but scaled linearly over a 100-fold range of electrical stimulus intensities (Fig. 3 *E*). Stimuli exceeding 200–300 μA produced hydrodynamic artifacts and hastened cellular death.

Vertical response of the cochlear partition to electrical stimuli

The vertical velocities of the tectorial and basilar membranes were recorded in response to electrical stimulation (Fig. 4 *A*). One-kilohertz, 30-μA sinusoidal stimuli elicited responses somewhat similar to those achieved with acoustic stimuli. On the tectorial membrane's upper surface, the vertical displacement was minimal closest to the spiral lamina and increased toward the spiral ligament (Fig. 4 *B*). Upward vertical velocity of the tectorial membrane lagged positive polarization of the upper compartment by ~90° (Fig. 4 *C*). In response to the same stimulus, the basilar membrane displayed a small but significant vertical displacement (Fig. 4 *D*).

Although the phase of the tectorial membrane's movement was constant across the radial dimension, the basilar membrane's response acquired a progressive phase advance toward the spiral ligament, with the outermost measurable

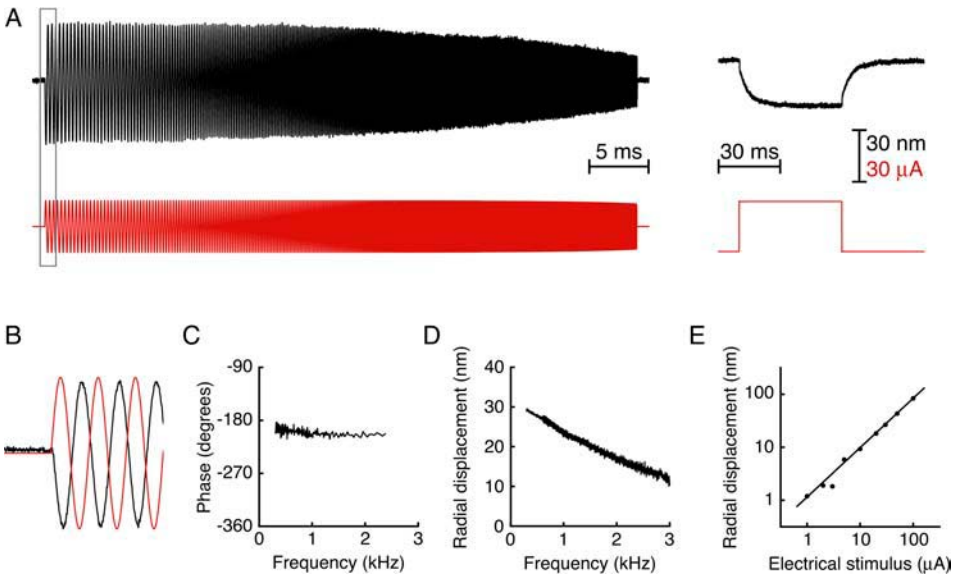

FIGURE 3 Electrically evoked movement of the cochlear partition. (*A*) The displacement of the hair bundle on an inner hair cell (*black*) was recorded in response to a 30-μA transepithelial current stimulus (*red*) in the form of a 300–3000 Hz frequency sweep (*left*) or a 50-ms pulse (*right*). Upward deflections correspond to positive polarization of the upper compartment and inward hair-bundle displacement toward the modiolus, which was accompanied by outward, or positive, bundle deflection toward the tallest row of stereocilia. (*B*) An overlay plot of the low-frequency end of the frequency-sweep stimulus and mechanical response reveals that positive polarization of the upper compartment was in phase with hair-bundle displacement away from the modiolus, or negative hair-bundle deflection. (*C*) The phase spectrum of inward hair-bundle displacement relative to positive upper-compartment polarization demonstrates a consistent phase difference slightly in excess of ~180° across the entire range of frequencies. (*D*) The frequency spectrum displays no resonant behavior. The gradual attenuation of displacement amplitude with increasing frequency likely reflects passive electrical filtering. (*E*) Hair-bundle displacement scaled linearly with the electrical stimulus over a range of 40 dB, with a power-law slope of 0.96 ($r^2 = 1.00$; note the logarithmic axes).

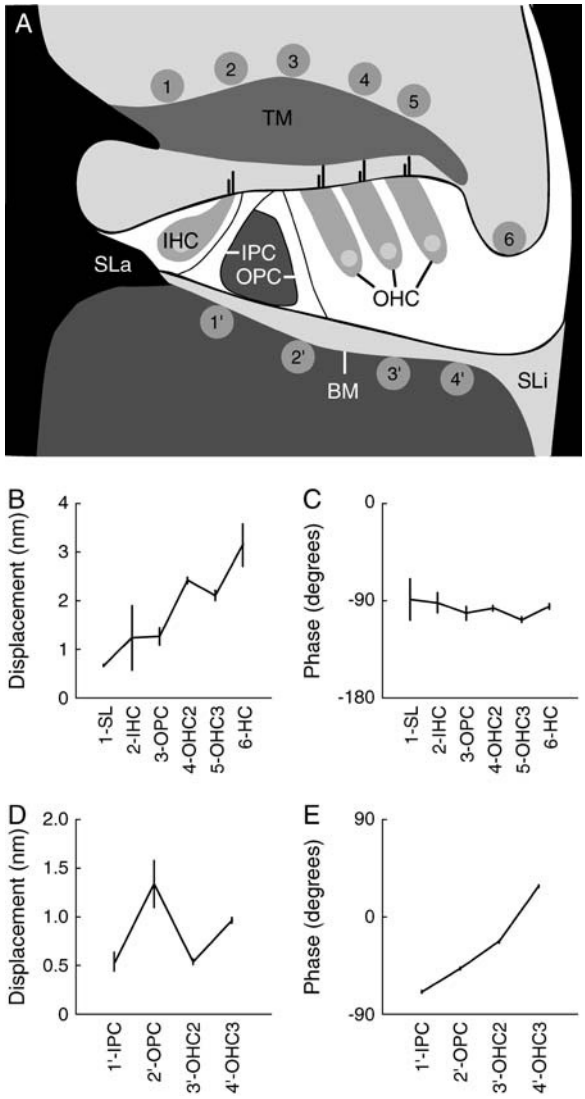

FIGURE 4 Vertical response of the cochlear partition to electrical stimuli. (*A*) The velocity of glass beads attached to the tectorial and basilar membranes was measured by laser Doppler interferometry. Numbers correspond to the locations indicated in *B–E*. (*B*) In response to a 1-kHz, 10-μA transepithelial electrical stimulus, tectorial-membrane displacement largely increased as a function of distance from the spiral lamina. (*C*) The phase of upward tectorial-membrane velocity did not vary significantly with radial position, and consistently lagged the electrical stimulus by 90°, indicating that downward displacement of the tectorial membrane was in phase with positive polarization of the upper compartment. (*D*) In response to a 1-kHz, 30-μA electrical stimulus, basilar-membrane displacement was limited and displayed no apparent radial trend. (*E*) In contrast to the tectorial-membrane results, the phase of upward basilar-membrane velocity varied substantially with radial position. The innermost position lagged the electrical stimulus by almost 90°, whereas the upward velocity of the outermost position, below the outer hair cells, was nearly in phase with the electrical stimulus. In general, however, the basilar membrane moved toward the scala tympani in response to positive polarization of the upper compartment. (*BM*, basilar membrane; *IHC*, inner hair cell; *IPC*, inner pillar cell; *OHC*, outer hair cell; *OPC*, outer pillar cell; *SLa*, spiral lamina; *SLi*, spiral ligament; and *TM*, tectorial membrane.) The points and vertical bars in *B–E* represent the means and standard deviations of the measurements.

point leading the innermost point by ~90° (Fig. 4 *E*). This phase lead was most dramatic in two preparations in which the outermost points actually moved in antiphase to the innermost points, as has been observed during electrical stimulation of the excised cochlear partition (11). Stimulation with current pulses yielded unambiguous response polarities, which confirmed that the tectorial membrane and basilar membrane responded as reported above: both structures moved away from the compartment that was positively polarized.

The motion of the tectorial membrane was significantly larger than the movement of the basilar membrane across the entire radial dimension. Unlike the response elicited acoustically, the electrically evoked response is not subject to hydrodynamic filtering, as indicated by its failure to exhibit any system-related resonances. Thus, the greater response of the tectorial membrane compared to the basilar membrane likely represents accurately the different effects of the electromechanical force on these two structures.

Radial response of the reticular lamina to electrical stimulation

Unlike the electrically evoked vertical response of the cochlear partition, which largely resembled the acoustic response, the radial movements of reticular-lamina structures were quite different for electrical and acoustic stimulation. The preparation was excited either with electrical pulses, which gave rise to sustained responses of clear polarity, or with frequency sweeps, which provided detailed phase information.

For both types of stimulation, a complex, trimodal response was seen in the radial dimension, with lines of inflection at the inner pillar cells and the first row of outer hair cells (Fig. 5, *A* and *B*). The hair bundles of the inner hair cells and the boundaries of the third row of outer hair cells moved in phase with each other, but in antiphase to intervening structures (Fig. 5 *C*). Although these inflections were seen consistently, their precise location varied slightly from one preparation to another. This may have reflected differences in the angle at which the preparations were mounted or authentic variations in their behavior. Stimulation with frequency sweeps revealed that these phase differences persisted across the entire frequency range of 300–3000 Hz.

Stroboscopic video microscopy of the electrically stimulated cochlear partition

Electrically evoked mechanical motion of the cochlear partition was imaged directly by stroboscopic video microscopy. Stimulation with a current of 50–100 μA, higher than the 10–30 μA usually employed, was necessary to elicit movements large enough for direct visualization. The response to electrical stimulation at 1000 Hz was observed under strobed illumination at ~1002 Hz (Supplementary Material, Fig. S3).

In corroboration of measurements made with the photodiode micrometer and with the laser interferometer, the

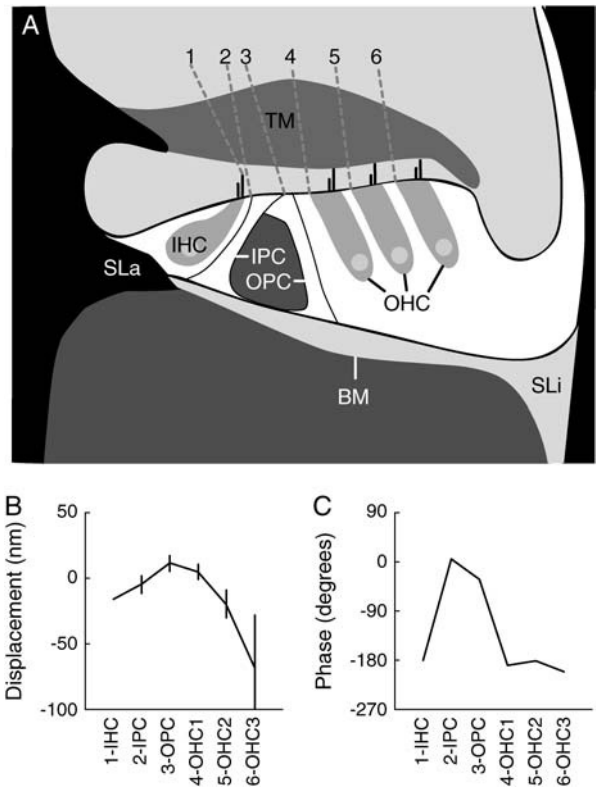

FIGURE 5 Radial response of the reticular lamina to electrical stimulation. (*A*) The displacements of the cellular structures on the reticular lamina indicated by dashed lines were measured with the photodiode projection system. In this instance, the inner edge of the inner pillar cells was also monitored. Numbers correspond to the locations indicated in *B* and *C*. (*B*) Displacements were measured in response to electrical pulses to provide an unambiguous polarity for each response. For the ordinate, positive displacement corresponds to radially inward movement, which reflects outward (positive) hair-bundle deflection, in response to 30-μA positive polarization of the upper compartment. (*C*) Frequency-sweep stimuli were used in a different preparation to obtain a more precise phase profile. The phase of radially inward displacement is given relative to the phase of positive polarization of the upper compartment. This result represents a single representative preparation; the precise location of the phase inflections varied slightly from one cochlea to another, but occurred consistently within this intermediate region. (*BM*, basilar membrane; *IHC*, inner hair cell; *IPC*, inner pillar cell; *OHC*, outer hair cell; *OPC*, outer pillar cell; *SLa*, spiral lamina; *SLi*, spiral ligament; and *TM*, tectorial membrane.) The points and vertical bars in *B* represent the means and standard deviations of the measurements.

vertical displacements of the tectorial and basilar membranes appeared substantially smaller than the radial displacement of the reticular lamina. Furthermore, structures at the level of the reticular lamina displayed a complex pattern of movement. Optical-flow analysis and direct observation of videos of the hair bundles on inner hair cells revealed that their deflection occurred against the background of a relatively stationary reticular lamina (Supplementary Material, Fig. S3; Fig. 6 *A*). This pattern suggests that the transepithelial electrical stimulus directly drives movement of these hair bundles, as has been demonstrated in the bullfrog's sacculus (19). In addition, the outer hair cells appeared to be changing their cross-sectional area, suggesting that somatic electromotility was also excited in this preparation. Analysis of optical flow on a broader spatial scale confirmed that electrical stimulation elicited a complex mode of radial vibration (Fig. 6, *B–D*): a clear line of inflection was visible at the level of the pillar cells, with structures on either side moving in opposite directions. In contrast, acoustic stimulation of the same preparation elicited radial movement in the same direction throughout the epithelium, confirming the simple, unimodal response described earlier (Fig. 6, *E* and *F*).

Geometrical gain factors in cochlear micromechanics

This preparation afforded an opportunity for the simultaneous or sequential measurement of the movements of the basilar membrane, tectorial membrane, and hair bundles under identical experimental circumstances and during acoustic stimulation near the natural frequency of the cochlear partition. As a consequence, we were able to quantify in several instances the geometrical gain, also termed the mechanical advantage or transformer ratio, characterizing the relative motion of one constituent of the cochlear partition with respect to another.

Sequential recordings in the same preparation near the first row of outer hair cells show that the ratio of vertical movement of the tectorial membrane to radial displacement of the reticular lamina was approximately one-third. Likewise, we found that the radial displacement of the outer pillar cell's boundary on the reticular lamina was ~70% of the maximal vertical movement of the basilar membrane. If the basilar membrane is assumed to vibrate in a circular arc, the average motion of the basilar membrane, which is the relevant value when considering the geometric gain in the context of the cochlear partition's vibration, is ~70% that of the maximal value. The geometrical gain of hair-bundle deflection with respect to average basilar-membrane motion ($\gamma_{HB/BM}$) was thus approximately unity. Finally, as assessed in a single exceptional preparation that permitted interferometric recording from both structures in the same recording configuration, the geometrical gain of the tectorial membrane with respect to the basilar membrane ($\gamma_{TM/BM}$) was approximately one-sixth. This ratio was roughly corroborated by indirect comparison of low-frequency asymptotic displacements measured at the tectorial and basilar membranes in other preparations, which yielded an average value of one-third. The geometrical gains estimated here are comparable to those suggested by modeling (20) and measured in the hemicochlea (21).

Stiffness of the cochlear partition and its components

When a pressure difference is applied across the cochlear partition, this stimulus is opposed in part by the stiffness of

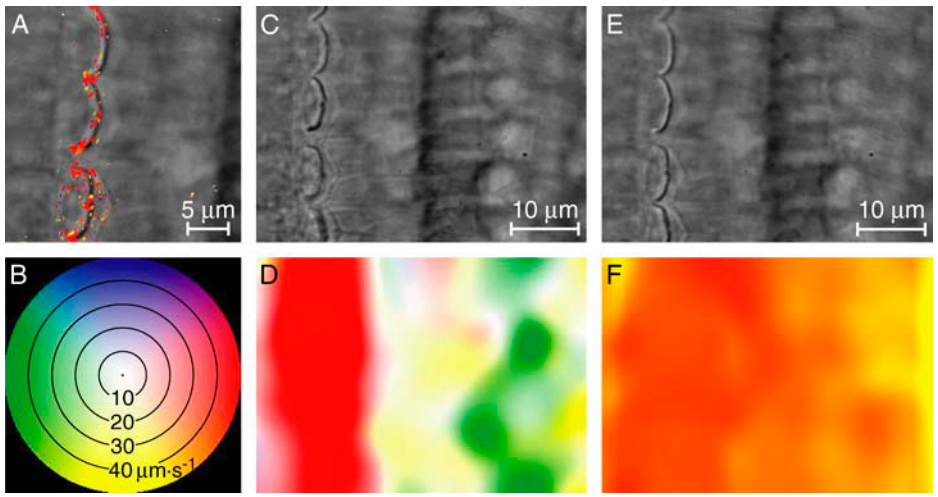

FIGURE 6 Stroboscopic video analysis of electrically and acoustically evoked motion. (*A*) A 50-μA, 1-kHz sinusoidal electrical stimulus elicited movement of the hair bundles atop inner hair cells against a nearly stationary background. Superimposed upon a differential-interference-contrast image frame captured from a stroboscopic video (Supplementary Material, Fig. S3) is the optical flow field determined with the parameter values $\sigma_S = 1.5$, $\sigma_T = 1$, $\tau = 1$, $\sigma_W = 1$, and $\rho = 0.02$. The red highlights correspond to radially outward movement of the hair bundles (to the right) at $\sim$16 μm $\cdot$ s^{-1}. (*B*) This pseudocolor scale calibrates the optical flow calculated with the Lucas-Kanade algorithm. Each color in *D* and *F* corresponds to motion in the direction indicated by the hue in this scale and at a speed indicated by the corresponding saturation. (*C*) A differential-interference-contrast image displays the preparation in *A* under the same electrical-stimulation conditions. (*D*) Optical-flow measurements reveal opposing directions of movement across the reticular lamina, with a line of inflection occurring at the pillar cells. The image was acquired at the phase of greatest basilar-membrane velocity toward the lower compartment. At this phase of stimulation, the apical surfaces of the inner hair cells moved radially outwards (*to the right*) at $\sim$50 μm $\cdot$ s^{-1}, whereas the tops of the first row of outer hair cells translated toward the modiolus (*to the left*) at a similar speed. The image was acquired at the phase of greatest basilar-membrane velocity toward the lower compartment. (*E*) Differential-interference-contrast microscopy shows the same preparation during subsequent acoustic simulation. (*F*) Optical-flow measurements indicate that acoustic stimulation elicited reticular-lamina motion that was in the same direction, radially outwards (to the right), throughout the field of view. The optical-flow parameter values for *D* and *F* were $\sigma_S = 1$, $\sigma_T = 1$, $\tau = 0.2$, $\sigma_W = 25$, and $\rho = 0.05$.

the basilar membrane (K_{BM}). The stimulus is also communicated mechanically to the tectorial membrane and hair bundles, whose deflection provides additional restoring forces. Because the tectorial membrane is thought to respond only to force transmitted through the hair bundles, these two structures lie in series with each other; the combination lies in parallel with the basilar membrane (22). As measured through resonance of the cochlear partition, the tectorial membrane and hair bundles contribute effective stiffnesses of K'_{TM} and K'_{HB}, respectively. The tectorial membrane's effective stiffness is the product of its actual stiffness, K_{TM}, and the square of its geometrical gain. The effective hair-bundle stiffness includes contributions from N bundles, each of stiffness K_{HB}, again weighted by the geometrical gain. The overall stiffness of the cochlear partition (K_{CP}) is therefore

$$K_{CP} = K_{BM} + \frac{K'_{HB}K'_{TM}}{K'_{HB} + K'_{TM}} = K_{BM} + \frac{(N\gamma^2_{HB/BM}K_{HB})(\gamma^2_{TM/BM}K_{TM})}{N\gamma^2_{HB/BM}K_{HB} + \gamma^2_{TM/BM}K_{TM}}. \quad (7)$$

We measured the stiffness of the cochlear partition by stimulating with acoustic frequency sweeps at frequencies of 300–3000 Hz and using a photodiode micrometer to measure the radial displacement of the hair bundles atop inner hair cells. The response typically exhibited a single major resonant peak that was fitted well by a Lorentzian relation (13). After determining the resonant frequency with different amounts of perilymph in the lower compartment of the experimental chamber, we used Eq. 6 to estimate the stiffness of the isolated segment of the cochlear partition as 20.0 $\pm$ 1.2 N $\cdot$ m^{-1} ($n = 7$ cochleae).

To assess the contributions of the tectorial membrane and the hair bundles, we measured the stiffness before and after removal of the tectorial membrane. In four such preparations, the stiffness of the intact cochlear partition averaged 18.5 $\pm$ 1.7 N $\cdot$ m^{-1}; removal of the tectorial membrane reduced this to 12.9 $\pm$ 0.8 N $\cdot$ m^{-1}, which differs significantly ($P < 0.02$, Student's paired *t*-test). The value determined after tectorial-membrane removal likely represented a direct measurement of the stiffness of the basilar membrane and organ of Corti alone. The difference between this value and the stiffness of the intact cochlear partition then represented a parallel stiffness of 5.6 N $\cdot$ m^{-1} attributable to the tectorial membrane and the hair bundles that connect it to the reticular lamina. The tectorial membrane and hair bundles lie in series, so their individual stiffness contributions—that is, the effective stiffnesses of the entire exposed segment of tectorial membrane and of all of the hair bundles in the preparation—each exceeded 5.6 N $\cdot$ m^{-1}.

Because the geometrical gain of tectorial-membrane motion with respect to basilar-membrane displacement was no more than one-third, the stiffness of the tectorial membrane, calculated from its effective contribution of at least 5.6 N $\cdot$ m^{-1}, exceeded 50 N $\cdot$ m^{-1}. The geometrical gain of hair-bundle displacement with respect to average basilar-membrane motion was approximately unity, hence the value

of 5.6 N · m^{-1} also provided an upper estimate of the effective hair-bundle stiffness. Assuming that all of the ~400 hair bundles in the preparation were coupled to the tectorial membrane and contributed in parallel to the aggregate hair-bundle stiffness, then the stiffness of a single hair bundle was 14 mN · m^{-1}.

Contribution of tip links to the stiffness of the cochlear partition

In the bullfrog's sacculus, the hair bundle's stiffness is dominated by that of the proteinaceous tip links that connect the tips of neighboring stereocilia and transmit force to mechanically gated transduction channels (23). To assess the contribution of the tip links to the stiffness of the cochlear partition in this mammalian preparation, we determined the stiffness before and after treatment with 1,2-bis(2-aminophenoxy)ethane-*N*,*N*,*N*′,*N*′-tetraacetic acid (BAPTA), which severs these tip links (24), and again after removal of the tectorial membrane (Fig. 7, *A* and *B*). As measured by linear regression fit of the perilymph's mass and ω_0^{-2}, the initial stiffness of one preparation was 19.5 N · m^{-1} ($r^2 = 0.97$). A 10-min treatment with 5 mM BAPTA decreased the value to 11.9 N · m^{-1} ($r^2 = 0.95$). Subsequent removal of the tectorial membrane diminished the stiffness still further, to 11.0 N · m^{-1} ($r^2 = 0.98$). If the stiffnesses were instead calculated for each measurement after determination of the perilymph's mass, these respective values were 20.3 ± 2.9 N · m^{-1}, 16.8 ± 3.7 N · m^{-1}, and 14.6 ± 2.9 N · m^{-1} ($n = 12$ measurements under each condition). The stiffness measured in the presence of the tectorial membrane and intact tip links differed significantly from both of the other values ($P < 0.05$, Student's unpaired *t*-test). The stiffness change was irreversible upon washout of the BAPTA solution with artificial endolymph (data not shown). By confirming that the stiffness change was not dependent upon the continuing presence of Ca^{2+} chelator, this result accorded with the expectation that the chelator disrupted tip links.

With identical amounts of perilymph present in the lower compartment, BAPTA treatment and subsequent tectorial-membrane removal each decreased the frequency and sharpness of the resonance peaks (Fig. 7, *C* and *D*). Comparison across six preparations corroborated the results from individual experiments: BAPTA treatment on average lowered the stiffness of the intact preparation by 25 ± 21%, and removal of the tectorial membrane reduced the stiffness by another 5 ± 11%. In these experiments, the stiffness in the intact preparation differed significantly from those obtained after tip-link disruption and tectorial-membrane removal ($P < 0.05$ for each, Student's paired *t*-test).

Because BAPTA's most significant effect on hair-bundle structure is the disruption of tip links (24), these results suggest that ~80% of the hair bundle's stiffness lies in the tip links and other elastic structures in series with them. A similar conclusion has been reached for the hair cells of the bullfrog's sacculus (23). As is the case for movements of the otolithic membrane in the sacculus (25), the elasticity of the gating springs therefore dominates the elastic reactance to shear between the reticular lamina and tectorial membrane. BAPTA also disrupts the basal links that connect adjacent stereocilia (26), structures that have been suggested to contribute significant stiffness in chick vestibular hair cells (27), but whose importance in mammalian cochlear hair cells has not been assessed. Because our preparations probably varied considerably in the extent of trauma inflicted upon their hair bundles and tip links—indeed, occasional preparations exhibited no change in stiffness with these treatments—these values likely underestimate the contributions of the hair bundles and tectorial membrane to the stiffness of the cochlear partition at acoustic frequencies in vivo.

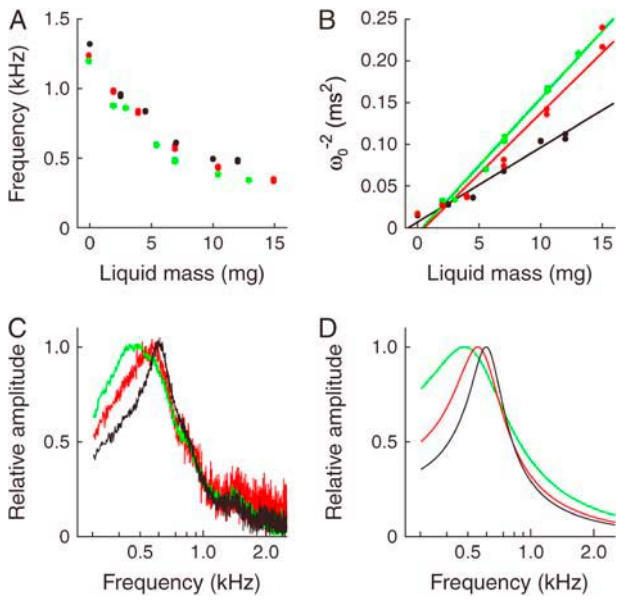

FIGURE 7 Stiffness of the cochlear partition. (*A*) The resonant frequency of the displacement response of the hair bundle on an inner hair cell was measured with varying total amounts of perilymph in the lower compartment in a freshly dissected preparation in the presence of K^+ endolymph (*black*); after a 10-min treatment with 5 mM BAPTA (*red*), which destroys tip links; and again after removal of the tectorial membrane (*green*). Each of these two treatments was found to decrease the resonant frequency. The same color code applies to the remaining panels. (*B*) The slopes of the mass-frequency relations from the data in *A* indicate that the stiffness of the cochlear partition was decreased sequentially by BAPTA treatment and tectorial-membrane removal. In K^+ endolymph, this stiffness was 19.5 N · m^{-1}; BAPTA treatment reduced it to 11.9 N · m^{-1}, and tectorial-membrane removal lowered it further, to 11.0 N · m^{-1}. (*C*) Frequency spectra of the hair bundle's displacement response with a 7-mm column of perilymph in the lower compartment demonstrate both downward shifts in the resonant frequency (f_0) and decreases in the quality factor (Q_0) after BAPTA treatment and then tectorial-membrane removal. (*D*) Lorentzian fits to the data of *C* emphasize the effects. In the presence of K^+ endolymph, the data yielded values of $f_0 = 612$ Hz and $Q_0 = 2.6$; BAPTA treatment lowered these to $f_0 = 558$ Hz and $Q_0 = 1.9$, and tectorial-membrane removal decreased them further to $f_0 = 482$ Hz and $Q_0 = 1.1$. In *C* and *D*, the response amplitude is normalized to the peak value for each condition.

DISCUSSION

Acoustically evoked movements of the cochlear partition

During acoustic stimulation, the techniques of photodiode micrometry, laser interferometry, and stroboscopic video microscopy revealed that the basilar membrane, tectorial membrane, and reticular lamina move nearly in phase with one another across their entire width at frequencies from 300 Hz to 3000 Hz. This finding suggests that the cochlear partition moves primarily as a rigid plate, pivoting along its insertion along the spiral lamina, without a line of inflection beneath the outer pillar cells (6). In agreement with findings of single-mode basilar-membrane motion (3–5), the vertical displacement is maximal at the most radial position accessible, near the lateral edge of the tectorial membrane and beneath the third row of outer hair cells. Whereas the reticular lamina exhibited significant radial motion, the tectorial membrane did not. As observed previously in the hemicochlea preparation (21), this arrangement provides a shear stimulus for the hair bundles. Because the shear stiffness of the tectorial membrane exceeds the rotational stiffness of the hair bundles (28), reticular-lamina displacement is likely to be transmitted almost completely to hair-bundle deflection.

Stroboscopic video microscopy permits subcellular resolution of cochlear-partition movement at high frequencies. Although direct, real-time observation of strobed videos generally requires high-intensity acoustic stimuli, more advanced optical-flow techniques can be used to detect lower-amplitude movements. Together with three-dimensional reconstruction, these methods may provide a comprehensive view of cochlear micromechanics at acoustic frequencies. Although such an approach has proven successful in the alligator lizard (29), the only study in which acoustically evoked movement in the mammalian cochlea has been observed using a comparable technique involved confocal imaging of fluorescently labeled cellular membranes in a passive preparation of the isolated temporal bone (30). In addition to displaying nonlinear amplification, the current in vitro preparation offers the advantage of subcellular resolution without the need for fluorescent labeling.

Comparison of acoustically and electrically evoked responses

Electrical stimuli have been used to elicit high-frequency movement of the cochlear partition under in vitro conditions that preclude acoustic stimulation (7,10,11). Such studies endeavored to reveal cochlear micromechanics under circumstances in which subcellular structures were readily visible. The relevance of these investigations, though, rests on the premise that electrically and acoustically evoked responses are equivalent, or at least comparable. In view of the strong coupling between hair-bundle movement, shear between the tectorial membrane and reticular lamina, and vertical vibration of the basilar membrane, one might expect electromechanical forces produced by hair bundles to induce movements of the cochlear partition that resemble acoustically driven ones. For soma-derived responses, however, the situation is less clear; electromotile changes in hair-cell length might not elicit cochlear-partition movement that resembles acoustically evoked motion. Our data provide an opportunity to compare responses to acoustic and electrical stimulation under identical conditions (Fig. 8).

In this preparation, the tectorial membrane and basilar membrane move in phase upon electrical stimulation. Together with previous pharmacological results (13), this finding suggests that electromechanical transduction in the presence of NMDG endolymph is dominated by force production in the hair bundle. Three notable differences between the responses of the cochlear partition to acoustic and electrical stimuli imply the additional operation of a soma-based mechanism. First, whereas the tectorial membrane's response to acoustic stimulation is no more than one-third that of the basilar membrane, the magnitude of the response to electrical stimulation on the tectorial membrane's surface is approximately fourfold that of the basilar membrane. Second, whereas a $\sim 90°$ phase lead accumulates in the basilar membrane's vertical response to electrical stimuli as the measurement progresses radially outward, no such phase difference is observed for the acoustically evoked response. The attenuated motion and phase profile of the basilar membrane probably reflect a conflation of bundle- and soma-based electromechanical transduction.

The most dramatic difference, however, lies in the radial response of intermediate structures along the reticular lamina. With acoustic stimulation, upward movement of the basilar and tectorial membranes is accompanied by an inward motion of all the structures across the reticular lamina, with the greatest excursion occurring near the spiral lamina. In the electrical response, by contrast, a region near the pillar-cell heads moves in antiphase, translating outward during upward movement. Moreover, the magnitude of radial displacement increases with distance from the spiral lamina. Soma-based electromotile force might set structures on either side of the outer hair cells into opposing motion even as a hair-bundle-based mechanism dominates the overall motion of the cochlear partition.

The differences between the acoustically and electrically evoked responses undoubtedly reflect the different sources of force in the two conditions, which are respectively pressure applied uniformly across the cochlear partition, and a combination of hair-bundle- and soma-based forces produced by outer hair cells. Detailed knowledge of the current pathway involved in electrical stimulation is required to interpret the responses it elicits. Although endolymph based on NMDG instead of K^+ was used exclusively in this study, this solution is not expected to have affected hair-bundle-based electromechanical transduction, which is driven by the Ca^{2+} current that persists under such conditions (13). The use of

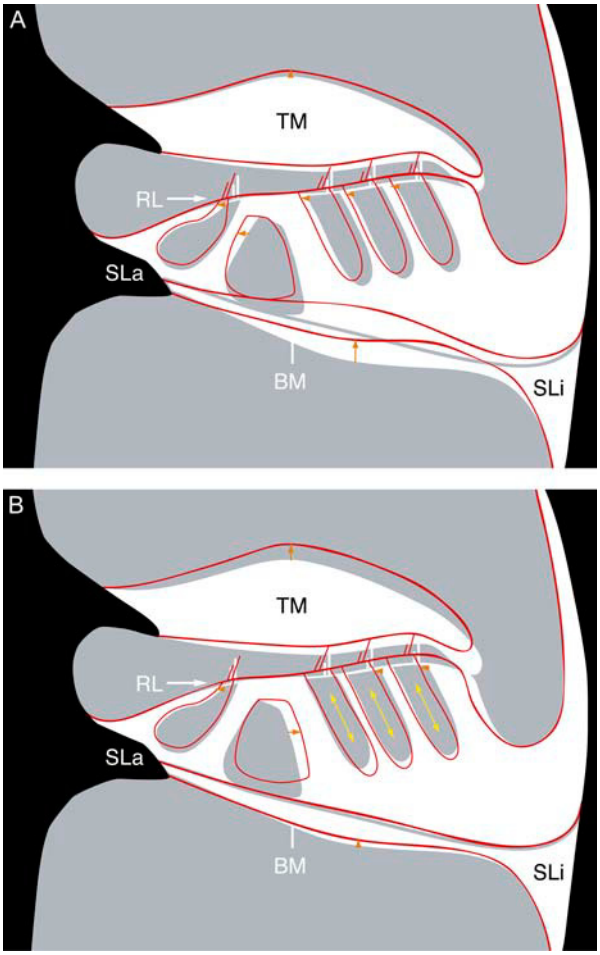

FIGURE 8 Motion of the cochlear partition in response to acoustic and electrical stimulation. With an exaggerated distance scale, this schematic illustration depicts the movements inferred from the measurements made in this study. In each panel, the cochlear partition is shown white-on-gray at one extreme of its motion; the other extreme is displayed with a red outline. Orange arrows emphasize the directions and relative magnitudes of movement of specific structures. (*A*) In response to an acoustic stimulus in the form of increased pressure in the lower compartment, the cochlear partition moves upwards as a unit. The vertical movement of the basilar membrane (*BM*) exceeds that of the tectorial membrane (*TM*), and displacements at the reticular lamina (*RL*) occur toward the spiral lamina (*SLa*) at all points. Both the spiral lamina and spiral ligament (*SLi*) remain stationary. (*B*) In contrast, electrical stimulation elicits complex modes of motion within the cochlear partition. In response to positive polarization of the lower compartment, the cochlear partition moves upwards. In contrast to the acoustic response, the vertical motion of the tectorial membrane exceeds that of the basilar membrane. The direction of radial motion at the reticular lamina varies with location: whereas the innermost and outermost points are displaced toward the spiral lamina, an intermediate region moves toward the spiral ligament. Positive polarization of the lower compartment depolarizes the apical membrane and hyperpolarizes the basolateral membrane of each hair cell. The electrically evoked response depicted here is therefore likely to result from the simultaneous recruitment of electromechanical transduction forces in the form of outward deflections of hair bundles and elongation of outer-hair-cell somata (*yellow arrows*).

NMDG endolymph is unlikely to have abolished electromechanical transduction based in the cell soma, which is driven primarily by electrical current flowing across the basolateral membrane (10). Both motile processes should therefore be observable in this preparation. The results presented here support the simultaneous action of two distinct electrically evoked responses: a hair-bundle-driven process that results in movement that largely resembles the acoustic response, and a soma-driven process that underlies the differences between the acoustic and electrical responses.

Implications of cochlear micromechanics for auditory transduction

Accurate modeling of the cochlear partition's micromechanical behavior requires an understanding of its dominant stiffnesses, which are likely to include those of the basilar membrane, hair bundles, and tectorial membrane. The basilar membrane's stiffness has been estimated previously by measuring the point stiffness across its width (31–34). Although point deflection conflates several potential modes of deformation and is qualitatively dissimilar from in vivo stimulation by acoustic pressure, the expected bulk stiffness of the basilar membrane in this preparation can be estimated from these values.

At the cochlear location examined in this preparation, the average point stiffness (K_P) of the jird's basilar membrane, as measured with a 25-μm probe, is 0.10 N $\cdot$ m^{-1} (34). From this value can be derived the membrane's specific volumetric stiffness (K_{SV}), which, for plausible models of the shape of the basilar membrane's distortion in response to pressure, is

$$K_{SV} = \frac{K_P}{2.4 \cdot wd^2}, \tag{8}$$

in which w is the basilar membrane's width and d is the diameter of the probe's tip (32). In the region of the cochlea under consideration, the width of the basilar membrane is 200–250 μm (35), so the specific volumetric stiffness is $\sim 2.7 \times 10^{11}$ Pa $\cdot$ m^{-2}. Dividing this value by the length of the exposed segment of cochlear partition of $\sim$700 μm yields a volumetric stiffness (K_V) of 3.8×10^{14} Pa $\cdot$ m^{-3}. This value describes the volume displaced by a given pressure gradient. By taking into account the area of the exposed cochlear segment, we estimate the conventional stiffness (K) relating the linear displacement of the cochlear partition in response to a force applied across it as $\sim$12 N $\cdot$ m^{-1}.

Removal of the tectorial membrane or disruption of tip links with BAPTA rendered the cochlear partition more compliant; this accords with the previous finding that the stiffness of the basilar membrane, although substantial, is not the only contribution to the cochlear partition's stiffness (33): both the tectorial membrane and the hair bundles exhibit significant stiffness. The mechanical properties of the tectorial membrane have been examined in detail and can be

compared with these results. When excised from the mouse and mounted flat on a solid surface, the tectorial membrane displays a radial shear stiffness in response to stimulation with a 10 μm magnetic bead of 0.18 $N \cdot m^{-1}$, which is comparable to the point stiffness of the basilar membrane (28,36). In vivo, the tectorial membrane experiences a very different stimulus than does the basilar membrane: whereas the latter moves in response to a transverse pressure gradient, the tectorial membrane is driven by forces transmitted from the basilar membrane through the hair bundles. Because each hair bundle is of a size similar to that of the stimulus probe described above, and a hair bundle in vivo is likely to push on the tectorial membrane in a fashion similar to the magnetic bead, the stiffness measured in vitro is a reasonable estimate of that associated with the interaction of one hair bundle with the tectorial membrane. In this preparation, the interaction of some 400 hair bundles with the tectorial membrane would be expected to yield a tectorial-membrane stiffness near 70 $N \cdot m^{-1}$.

In this study, the stiffnesses of the basilar membrane and tectorial membrane for the 700-μm length of exposed cochlear partition were estimated as 12 $N \cdot m^{-1}$ and at least 50 $N \cdot m^{-1}$, respectively, which are closely comparable with previous findings. The estimated stiffness of an individual hair bundle, 14 $mN \cdot m^{-1}$, somewhat exceeds the values measured heretofore (32,33) by two techniques: either a hair bundle was deflected by a fluid jet (37,38), or it was pushed directly by a flexible fiber (39–41). Because the coupling between the stimulus and the hair bundle was not precisely characterized in the former instance, the force applied to the bundle had to be estimated, and the true bundle stiffness might have been underestimated. Direct stimulation with a glass fiber, on the other hand, might not have deflected all the stereocilia, especially in view of their weak lateral coupling (42). This would have likewise yielded an underestimate of the hair-bundle stiffness. Furthermore, the hair bundles examined previously in neonatal cochleae were immature, and those assessed in adult animals might not have retained their full complement of tip links after dissection, isolation, and strong stimulation. Estimates of hair-bundle stiffness from acutely isolated preparations with robust mechanoelectrical transduction reach 3–5 $mN \cdot m^{-1}$ (38,41), values approaching that measured here. Moreover, reducing the Ca^{2+} concentration to physiological levels increases the stiffness of hair bundles (23,41); adjusting the previous stiffness estimates for the normal endolymphatic Ca^{2+} concentration would nearly treble those values.

In these experiments, the hair bundles retained their insertions into the tectorial membrane and were stimulated en masse, thus recruiting a larger number of stereocilia than in previous studies. Together with the use of a low, endolymph-like Ca^{2+} concentration, this stimulus paradigm probably allowed the measurement of stiffnesses that are more relevant to in vivo conditions than have been obtained previously. The demonstrated presence of mechanoelectrical transduction and nonlinear amplification attest to the functional and structural integrity of the hair bundles in this preparation (13). Although uncertainty regarding the precise geometric gain between hair-bundle deflection and basilar-membrane motion, as well as uncharacterized effects at the fixed ends of the preparation, may have led to a misestimation of individual hair-bundle stiffness, the critical consideration in the contribution of hair bundles to cochlear-partition stiffness is the combination of their stiffness and geometric gain. This macroscopic stiffness contribution of the hair bundles was measured directly as 5.6 $N \cdot m^{-1}$, a value comparable to those of the basilar and tectorial membranes.

The correspondence between the stiffnesses of the basilar membrane, tectorial membrane, and hair bundles in the context of their mechanical interaction within the cochlear partition supports the notion that active forces generated by hair bundles can amplify movements of the basilar membrane. Much of the hair bundles' stiffness can be attributed to the BAPTA-sensitive tip links, which are situated so as to transfer force effectively to and from the mechanoelectrical transduction apparatus. Together with the ability of electrical stimuli to elicit substantial mechanical responses, this finding suggests that the cochlear partition's micromechanical properties facilitate the bidirectional propagation of motion. An active process based on the transduction channels themselves, or on the myosin motors that anchor the channels to the stereociliary actin cores, would therefore be able to drive movement of the cochlear partition and contribute to active amplification.

SUPPLEMENTARY MATERIAL

An online supplement to this article can be found by visiting BJ Online at http://www.biophysj.org.

The authors thank Mr. B. Fabella for computer programming and Mr. A. Hinterwirth for machining assistance. The members of our research group and two reviewers provided helpful comments on the manuscript.

This research was supported by grant No. DC00241 from the National Institutes of Health. A.J.H. is an Investigator of the Howard Hughes Medical Institute.

REFERENCES

1. de Boer, E. 1996. Mechanics of the cochlea: modeling efforts. *In* The Cochlea. P. Dallos, A.N. Popper, and R.R. Fay, editors. Springer-Verlag, New York. 258–317.
2. Robles, L., and M. A. Ruggero. 2001. Mechanics of the mammalian cochlea. *Physiol. Rev.* 81:1305–1352.
3. Cooper, N. 2000. Radial variation in the vibrations of the cochlear partition. *In* Recent Developments in Auditory Mechanics. H. Wada, T. Takasaka, K. Ikeda, K. Ohyama, and T. Koike, editors. World Scientific, Singapore. 109–115.
4. Rhode, W. S., and A. Recio. 2000. Study of mechanical motions in the basal region of the chinchilla cochlea. *J. Acoust. Soc. Am.* 107:3317–3332.

5. Richter, C. P., and P. Dallos. 2003. Micromechanics in the gerbil hemicochlea. *In* Biophysics of the Cochlea: From Molecules to Models. A.W. Gummer, editor. World Scientific, Singapore. 279–284.
6. Nilsen, K. E., and I. J. Russell. 1999. Timing of cochlear feedback: spatial and temporal representation of a tone across the basilar membrane. *Nat. Neurosci.* 2:642–648.
7. Reuter, G., A. H. Gitter, U. Thurm, and H. P. Zenner. 1992. High frequency radial movements of the reticular lamina induced by outer hair cell motility. *Hear. Res.* 60:236–246.
8. Xue, S., D. C. Mountain, and A. E. Hubbard. 1995. Electrically evoked basilar membrane motion. *J. Acoust. Soc. Am.* 97:3030–3041.
9. Nuttall, A. L., M. Guo, and T. Ren. 1999. The radial pattern of basilar membrane motion evoked by electric stimulation of the cochlea. *Hear. Res.* 131:39–46.
10. Scherer, M. P., and A. W. Gummer. 2005. Vibration pattern of the organ of Corti up to 50 kHz: evidence for resonant electromechanical force. *Proc. Natl. Acad. Sci. USA.* 101:17652–17657.
11. Mammano, F., and J. F. Ashmore. 1993. Reverse transduction measured in the isolated cochlea by laser Michelson interferometry. *Nature.* 365:838–841.
12. Ren, T., A. L. Nuttall, and J. M. Miller. 1996. Electrically evoked cubic distortion product otoacoustic emissions from Gerbil cochlea. *Hear. Res.* 102:43–50.
13. Chan, D. K., and A. J. Hudspeth. 2005. Ca^{2+} current-driven nonlinear amplification by the mammalian cochlea *in vitro*. *Nat. Neurosci.* 8: 149–155.
14. Hudspeth, A.J., and D.K. Chan. 2005. An experimental preparation of the mammalian cochlea that displays compressive nonlinearity *in vitro*. In Auditory Mechanisms: Processes and Models. A. L. Nuttall, editor. World Scientific, Singapore. In press.
15. Nowak, R. M. 1999. Walker's Mammals of the World, 6th Ed. The Johns Hopkins University Press, Baltimore, MD. 1344–1616.
16. Olson, E. 1999. Direct measurement of intra-cochlear pressure waves. *Nature.* 402:526–529.
17. Lucas, B., and T. Kanade. 1981. An iterative image registration technique with an application to stereo vision. Proceedings of the DARPA Image Understanding Workshop, Los Angeles, CA.
18. Abràmoff, M. D., W. J. Niessen, and M. A. Viergever. 2000. Objective quantification of the motion of soft tissues: an application to orbital soft tissue motion. *IEEE Trans. Med. Imag.* 19:986–995.
19. Bozovic, D., and A. J. Hudspeth. 2003. Hair-bundle movements elicited by transepithelial electrical stimulation of hair cells in the sacculus of the bullfrog. *Proc. Natl. Acad. Sci. USA.* 100:958–963.
20. Rhode, W. S., and C. D. Geisler. 1967. Model of the displacement between opposing points on the tectorial membrane and reticular lamina. *J. Acoust. Soc. Am.* 42:185–190.
21. Hu, X., B. N. Evans, and P. Dallos. 1999. Direct visualization of organ of Corti kinematics in a hemicochlea. *J. Neurophysiol.* 82:2798–2807.
22. Patuzzi, R. 1996. Cochlear micromechanics and macromechanics. *In* The Cochlea. P. Dallos, A.N. Popper, and R.R. Fay, editors. Springer-Verlag, New York. 186–257.
23. Marquis, R. E., and A. J. Hudspeth. 1997. Effects of extracellular Ca^{2+} concentration on hair-bundle stiffness and gating-spring integrity in hair cells. *Proc. Natl. Acad. Sci. USA.* 98:11923–11928.
24. Assad, J. A., G. M. Shepherd, and D. P. Corey. 1991. Tip-link integrity and mechanical transduction in vertebrate hair cells. *Neuron.* 7:985–994.
25. Benser, M. E., N. P. Issa, and A. J. Hudspeth. 1993. Hair-bundle stiffness dominates the elastic reactance to otolithic-membrane shear. *Hear. Res.* 68:243–252.
26. Goodyear, R., and G. Richardson. 1999. The ankle-link antigen: an epitope sensitive to calcium chelation associated with the hair-cell surface and the calycal processes of photoreceptors. *J. Neurosci.* 19: 3761–3772.
27. Bashtanov, M. E., R. J. Goodyear, G. P. Richardson, and I. J. Russell. 2004. The mechanical properties of chick (*Gallus domesticus*) sensory hair bundles: relative contributions of structures sensitive to calcium chelation and subtilisin treatment. *J. Physiol.* 559:287–299.
28. Freeman, D. M., C. C. Abnet, W. Hemmert, B. S. Tsai, and T. F. Weiss. 2003. Dynamic material properties of the tectorial membrane: a summary. *Hear. Res.* 180:1–10.
29. Aranyosi, A. J., and D. M. Freeman. 2004. Sound-induced motions of individual cochlear hair bundles. *Biophys. J.* 87:3536–3546.
30. Fridberger, A., and J. B. de Monvel. 2003. Sound-induced differential motion within the hearing organ. *Nat. Neurosci.* 6:446–448.
31. Gummer, A. W., B. M. Johnstone, and N. J. Armstrong. 1981. Direct measurement of basilar membrane stiffness in the guinea pig. *J. Acoust. Soc. Am.* 70:1298–1309.
32. Olson, E. S., and D. C. Mountain. 1991. *In vivo* measurement of basilar membrane stiffness. *J. Acoust. Soc. Am.* 89:1262–1275.
33. Naidu, R. C., and D. C. Mountain. 1998. Measurements of the stiffness map challenge a basic tenet of cochlear theories. *Hear. Res.* 124:124–131.
34. Emadi, G., C. P. Richter, and P. Dallos. 2004. Stiffness of the gerbil basilar membrane: radial and longitudinal variations. *J. Neurophysiol.* 91:474–488.
35. Plassmann, W., W. Peetz, and M. Schmidt. 1987. The cochlea in gerbilline rodents. *Brain Behav. Evol.* 30:82–101.
36. Abnet, C. C., and D. M. Freeman. 2000. Deformations of the isolated mouse tectorial membrane produced by oscillatory forces. *Hear. Res.* 144:29–46.
37. Géléoc, G. S., G. W. Lennan, G. P. Richardson, and C. J. Kros. 1997. A quantitative comparison of mechanoelectrical transduction in vestibular and auditory hair cells of neonatal mice. *Proc. R. Soc. Lond. B Biol. Sci.* 264:611–621.
38. van Netten, S. M., T. Dinklo, W. Marcotti, and C. J. Kros. 2003. Channel gating forces govern accuracy of mechano-electrical transduction in hair cells. *Proc. Natl. Acad. Sci. USA.* 100:15510–15515.
39. Strelioff, D., and Å. Flock. 1984. Stiffness of sensory-cell hair bundles in the isolated guinea-pig cochlea. *Hear. Res.* 15:19–28.
40. Kössl, M., G. P. Richardson, and I. J. Russell. 1990. Stereocilia bundle stiffness: effects of neomycin sulphate, A23187 and concanavalin A. *Hear. Res.* 44:217–230.
41. Kennedy, H. J., A. C. Crawford, and R. Fettiplace. 2005. Force generation by mammalian hair bundles supports a role in cochlear amplification. *Nature.* 433:880–883.
42. Langer, M. G., S. Fink, A. Koitschev, U. Rexhausen, J. K. H. Hörber, and J. P. Ruppersberg. 2001. Lateral mechanical coupling of stereocilia in cochlear hair bundles. *Biophys. J.* 80:2608–2621.